Thermochimica Acta, 203 (1992) 475–492
Elsevier Science Publishers B.V., Amsterdam

Cryomicroscopy as a support technique for calorimetric measurements by DSC for the study of the kinetic parameters of crystallization in aqueous solutions. Part 1. Nucleation in the water–1,2-propanediol system

Patrick M. Mehl

Transplantation Laboratory, J.H. Holland Laboratory for Biomedical Sciences, American Red Cross, 15601 Crabbs Branch Way, Rockville, MD 20855 (USA)

(Received 10 June 1991)

Abstract

Cryomicroscopy is shown to be complementary to calorimetry for qualitative and quantitative studies of crystallization kinetic parameters of aqueous solutions. The binary system water–1,2-propanediol is investigated as an example, using the Johnson–Avrami theoretical model under isothermal conditions. The effect of nucleation on crystallization parameters is discussed, comparing calorimetric measurements with direct observations by cryomicroscopy.

The experimental results depend strongly upon the thermal history of the sample prior to the isothermal experiment. The density of nuclei formed during warming after vitrification in 42.5% w/w 1,2-propanediol is inversely proportional to the warming rate, i.e. proportional to the time spent in the homogeneous nucleation thermal domain. The results support the hypothesis of a kinetic component for liquid–crystal phase separation during homogeneous nucleation.

Assuming an Arrhenius dependence for the crystallization constant, $K = K_0 \exp(-E/RT)$, K_0 is shown to vary as the square root of the nucleus density, in agreement with the discoidal form of the crystals; the activation energy E is shown to be independent of nucleus density.

INTRODUCTION

In order to be able to vitrify organs for the purpose of preserving them indefinitely at very low temperatures, new chemical or vitrification agents have to be defined [1,2]. However, a fundamental practical problem is to avoid crystallization during rewarming after vitrification. For relatively

Correspondence to: P.M. Mehl, Transplantation Laboratory, J.H. Holland Laboratory for Biomedical Sciences, American Red Cross, 15601 Crabbs Branch Way, Rockville, MD 20855, USA.

Dedicated to Professor Joseph H. Flynn in honour of his 70th birthday.

concentrated aqueous solutions, the temperature ranges for nucleation and for ice-crystal growth will overlap somewhat, as has been shown for 1,3-butanediol–water solutions at concentrations above 56% w/w (personal observation). For crystal growth the rate-limiting factor will be the viscosity of the solution. Nucleus formation is also dependent on diffusion although over shorter distances. The temperature range for crystal growth is always higher than that for nucleation, so that during cooling, nucleation may be invisible because of the absence of crystal growth. For this reason, vitrification is always easier to achieve during cooling than to preserve during rewarming. These factors complicate the modeling of the crystallization of ice in aqueous solutions, particularly during continuous warming.

Cryomicroscopy has already been used extensively with a cooling stage for studying the ice crystal growth in different aqueous solutions [3–6]. This technique has also been used previously by the author for the determination of nucleation and crystal growth for relatively concentrated solutions of 1,3-butanediol in order to study the mechanism of ice devitrification during warming [3,4]. To better understand the effect of different parameters on crystallization kinetics, especially on the nucleation process, we have found cryomicroscopy, as shown in the present paper to be both a qualitative and a quantitative technique complementary to differential scanning calorimetry (DSC). Isothermal experiments have been used to investigate the nucleation process in aqueous solutions of 1,2-propanediol which we use as a vitrification agent in cryoprotective solutions [7,8]. The theoretical Johnson–Avrami model is well known and is commonly used to describe the crystallization behavior in different liquid–crystal isothermal transformations [9]; we have utilized this theory to analyze our data acquired by DSC and by cryomicroscopy.

MEASUREMENTS

Aqueous solutions of 1,2-propanediol (Sigma) were prepared either with deionized water or with deionized water containing 6 g l^{-1} of Ice Nucleating Agent bacteria (INA), *Pseudomonas syringae* (Snowmax Technologies, Kodak, Inc.). All concentrations are expressed as % weight/weight.

Emulsions containing 1:1 methylcyclopentane (98% Aldrich)/methylcyclohexane (99% + Aldrich) were made using the technique of MacFarlane [10]; 4% w/w SPAN 65 (Sorbitan tristearate, Fluka) was then added as surfactant and mixed at a warm temperature to a homogeneous liquid [10,11]. The emulsions were prepared by passing the two solutions under pressure several times through a 26 gauge 1/2 inch needle on a 5 ml syringe.

Calorimetric measurements were made with a DSC-4 (Perkin–Elmer) using cooling and warming rates between 1 and 320°C min^{-1}. Thermal control, however, cannot be maintained for cooling rates above 80°C min^{-1}

[12]. The sample weight was between 5 and 12 mg. Samples without INA were filtered through 0.2 μm filters prior to experiments. Thermograms during both cooling and warming were recorded to measure the different thermal events.

Our cryomicroscopy system for direct optical measurements has been described previously [3–6]. Feed-back thermal control allows cooling rates of 40°C min^{-1} down to about −100°C and 20°C min^{-1} down to about −130°C. Warming rates of 1–99°C min^{-1} can be achieved. The 20 mm^3 sample solutions are placed between two 16 mm circular cover slips and placed in the field of the cryomicroscope. The direct optical observations are recorded with a VCR through a videocamera, providing a sample-to-TV-screen magnification of 500.

THEORY

The Johnson–Avrami model for isothermal conditions gives the relationship for the crystallization fraction X [13–16]

$$X = 1 - \exp\left(-(Kt)^n\right) \tag{1}$$

where t is the time of exposure, n the Avrami exponent depending on the geometry of the crystal and on the type of nucleation process, and $K = K_0 \exp(-E/RT)$, the crystallization constant, assuming an Arrhenius behavior even at temperatures close to the glass transition. This assumption is not valid for semi-fragile glasses such as the present binary system [17], but simplifies the calculation by limiting the number of parameters describing the crystallization process.

The method used is a derivative technique. Assuming isothermal conditions and that K is independent of t, the second time derivative of X gives

$$d^2X/dt^2 = (1-X)K^n t^{n-2} n\left((n-1) - n(Kt)^n\right) \tag{2}$$

By considering the time t_{max} at the maximum crystallization rate (dX/dt) which corresponds statistically to crystals beginning to overlap each other, this second derivative of X must be equal to zero, leading to a relationship which can be used for the determination of the different crystallization parameters

$$Kt_{max} = \text{constant} \quad \text{or} \quad t_{max} K_0 \exp(-E/RT) = \text{constant} \tag{3}$$

It is legitimate to assume that the nucleation might occur transiently during cooling and warming of the sample to the isothermal temperature T, and also during the exposure time at that temperature.

Two experiment sets were designed to study nucleation. In the first set, the temperature T was maintained and either the initial cooling rates or the subsequent warming rates were varied. In the second set, the cooling

and warming rates were maintained but the final temperature T was varied.

RESULTS

Phase diagram — comparison between cryomicroscopy and DSC

The phase diagram for the system water–1,2-propanediol was investigated using the emulsion technique which allows a separation of homogeneous and heterogeneous nucleation during cooling. The transitions are reported in Fig. 1. This technique has been elaborated by Charoenrein and Reid for aqueous solutions of sucrose [18]. The melting temperatures are also compared with those from the literature [19,20] with reported discrepancies of less than 2°C. The temperatures of homogeneous (T_{hom}) and heterogeneous (T_{het}) nucleation during cooling are shown. T_g^* is the glass transition temperature for the remaining amorphous state after the ice has

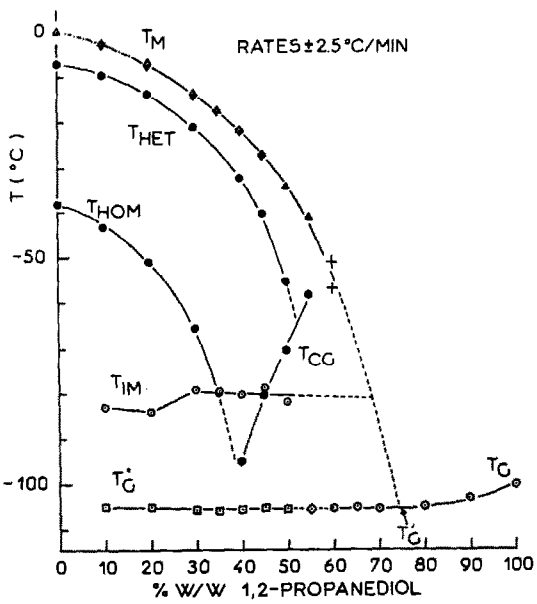

Fig. 1. Dynamic phase diagram for the binary system water–1,2-propanediol during cooling and warming at 2.5°C min^{-1} by calorimetry (DSC-4). This diagram is constructed from emulsion systems with samples containing ice nucleating agents (INA). T_m, melting temperature; T_{het} heterogeneous nucleation temperature; T_{hom}, homogeneous nucleation temperature; T_{cg}, temperature of the beginning of the devitrification during warming (crystal growth); T_g^*, glass transition temperature for the residual amorphous state after ice crystallization during cooling at 2.5°C min^{-1}; T_g, glass transition of the wholly vitreous state without any crystallization; T_{im}, incipient melting temperature. For the melting temperatures, data from the literature are reported from: (▼) ref. 19 and (·) ref. 20.

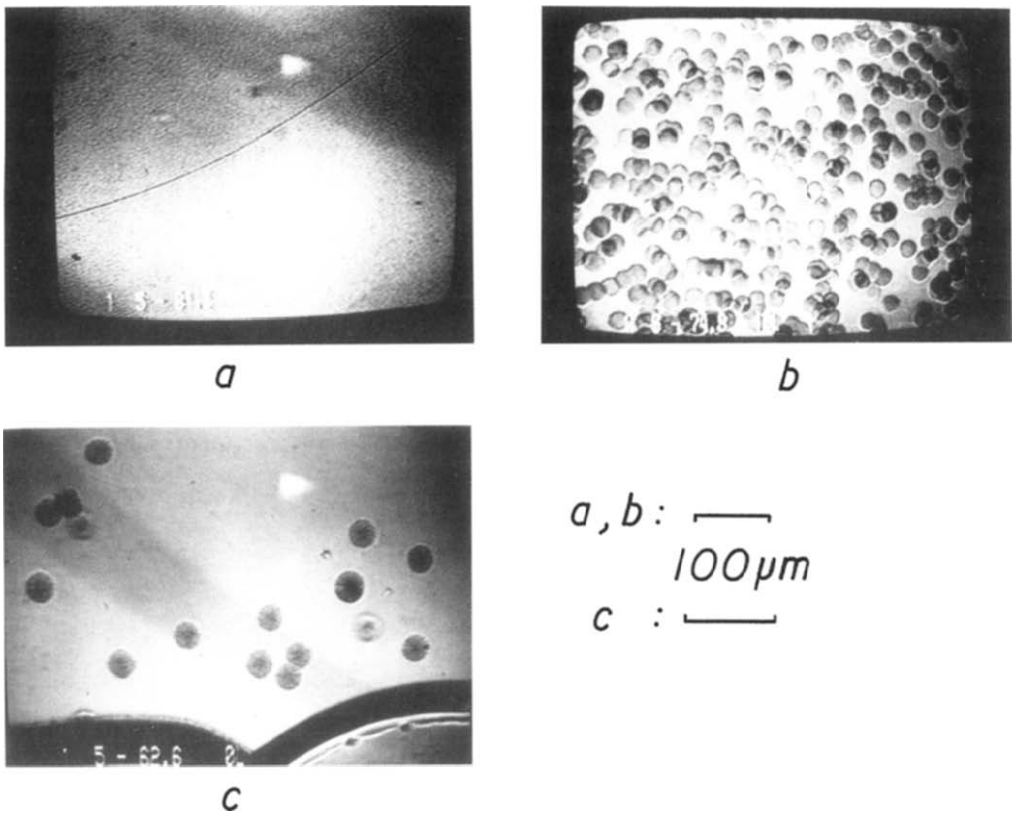

Fig. 2. Photos of samples of (a) 40%, (b) 42.5% and (c) 45% 1,2-propanediol cooled at 40°C min^{-1} to −160°C and warmed back at 5°C min^{-1} until ice crystallization. For 40%, homogeneous nucleation occurs with an "infinite" number of crystals (relative to the TV screen sensitivity); for higher concentrations this number decreases.

crystallized during cooling. T_g is the glass transition temperature for samples without INA which vitrify during cooling at 2.5°C min^{-1}. The temperature of crystal growth T_{cr} is the onset temperature for the devitrification peak during warming. T_{im} is the incipient melting temperature as described in ref. 21 which must be distinguished from the limiting glass transition [22].

Figure 2 illustrates crystallization in 40%, 42.5% and 45% 1,2-propanediol in water cooled at 40°C min^{-1} to −160°C and warmed back at 5°C min^{-1} to −10°C. Boutron and Kaufmann have shown that a cooling rate of 40°C min^{-1} is sufficient to vitrify samples of concentrations higher than 40% 1,2-propanediol [19]. Homogeneous nucleation is commonly described in the literature as an equilibrium process with the formation of an infinite number of nuclei. 40% 1,2-propanediol undergoes a homogeneous nucleation with numerous nuclei, but nucleation appears not to occur at concen-

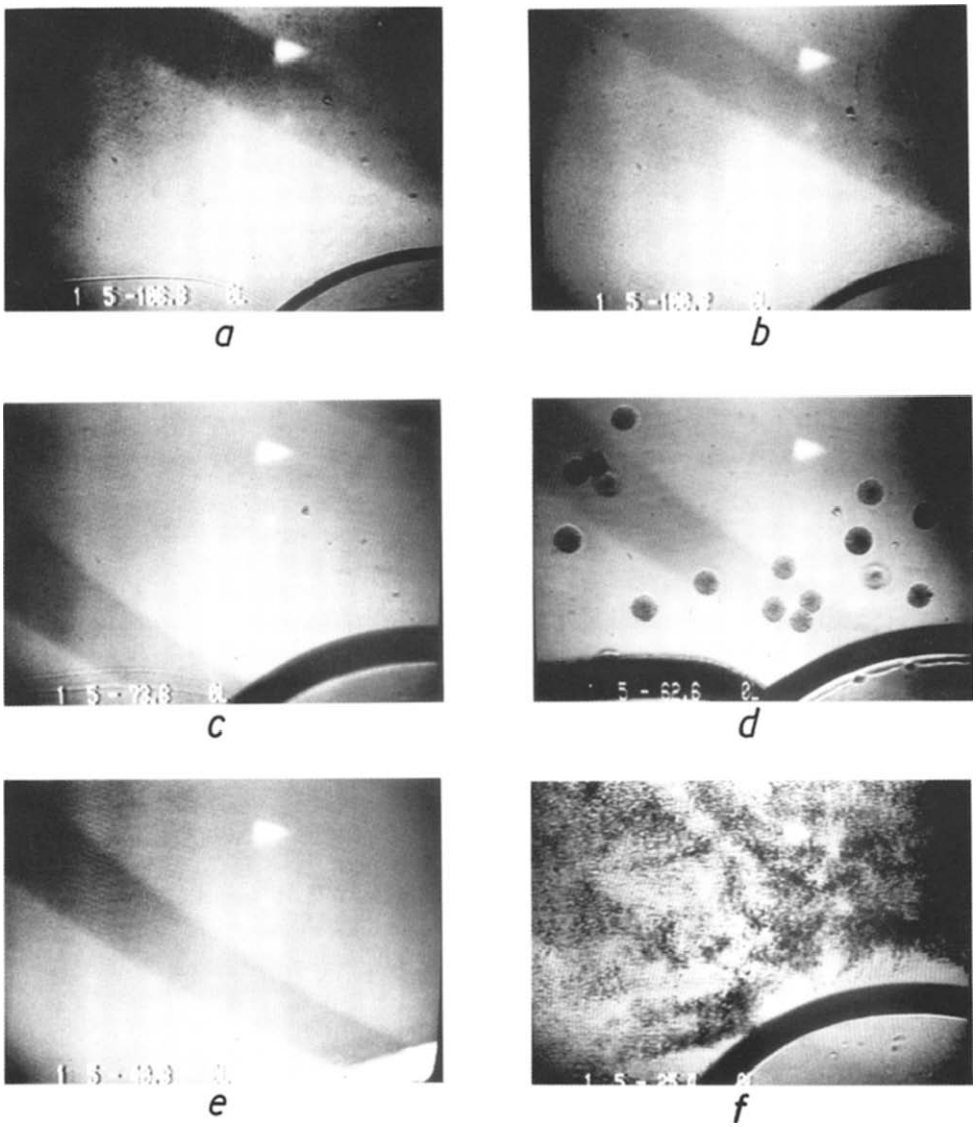

Fig. 3. Cryomicroscopic observations for a sample of 45% 1,2-propanediol cooled at 40°C min^{-1} to −160°C. Pictures are recorded during the warming back at 5°C min^{-1}. Cryomicroscopy observations: (a) beginning of the disappearance of the fractures created during cooling; (b) completed disappearance of the fracture from the TV screen; (c) reappearance of the fracture owing to crystal growth from the fracture; (d) crystal growth from isolated ice nuclei; (e) end of crystallization and apparent beginning of the melting process; (f) melting at 2°C before the end of melting.

trations above 42.5%. This correlates the extrapolation of the T_{hom} curve to the T_g curve giving an intersection between 40 and 45%. However, as will be discussed later, the term homogeneous nucleation is ill-defined in the case of these aqueous solutions and the number of nuclei forming must be determined.

Figure 3 presents micrographs of a 45% 1,2-propanediol sample cooled at 40°C min^{-1} to −160°C and warmed back at 5°C min^{-1} to −10°C. As the sample is cooled, nucleating fractures form as previously reported for other aqueous solutions [3–6]. Nucleation is presumably the result of local warming during propagation of the cracks and several authors have reported triboluminescence, triboemissions and local temperature increases associated with the cracking of glasses and other materials [23,24]. As the sample is warmed, molecular diffusion increases and near the glass transition temperature, the fractures disappear because of molecular diffusion into the fractures. The fractures reappear at higher temperatures as a result of the growth of ice from pre-existing nuclei. At higher temperatures, isolated nuclei form and grow. Crystal growth from both fracture edges and isolated nuclei can be directly observed. After completion of the growth, the medium is totally opaque because of the Ostwald ripening phenomenon. As the temperature rises further, the medium becomes increasingly transparent as melting of the ice progresses. All of these events can be seen in Fig. 4 which reproduces a recorded thermogram. There is an excellent and straightforward correlation between the direct cryomicroscopic observations and the thermal events recorded with the DSC-4.

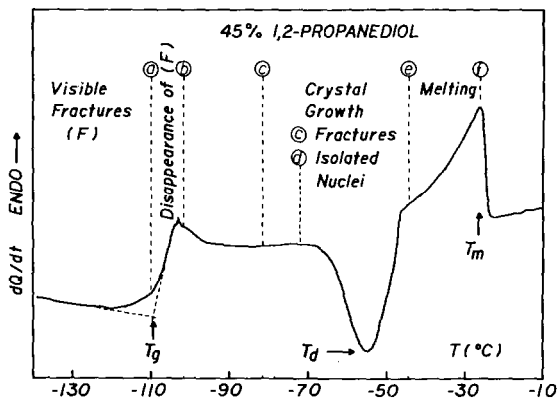

Fig. 4. Comparison of cryomicroscopy observations and DSC-4 thermal events for 45% 1,2-propanediol cooled at 40°C min^{-1} to −160°C and warmed back to −10°C at 5°C min^{-1}. The thermogram during warming from DSC is drawn in an arbitrary scale for the power dQ/dt. T_m, end of melting temperature; T_d, devitrification temperature; T_g, glass temperature. The cryomicroscopy observations correspond to those reported in Fig. 2. The temperatures are back-fitted assuming that both experiments have the same end of melting temperature.

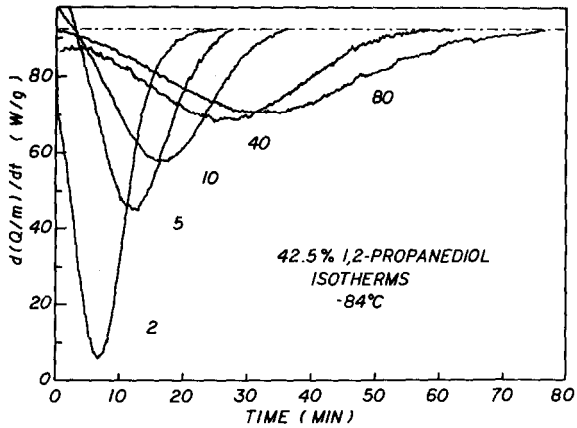

Fig. 5. Isothermal thermograms acquired by DSC-4 for 42.5% 1,2-propanediol in pure water. The sample is cooled at 40°C min^{-1} to −160°C avoiding any crystallization during cooling and warmed back at different rates (°C min^{-1}) reported on the side of each thermogram to the same temperature, −84°C. The ordinate scale is reported per gram of solution.

Application to nucleation

Two different isothermal experiments were performed. In Fig. 5, DSC isothermograms were recorded for samples of 42.5% 1,2-propanediol which were cooled at 40°C min^{-1} to −160°C and warmed back at different rates to the same temperature, −84°C, for the isothermal exposition. In Fig. 6, DSC isothermograms were recorded for samples which were cooled to −160°C and warmed at 40°C min^{-1} to different holding temperatures. Cryomicroscopic observations are reported in Fig. 7 for the same experi-

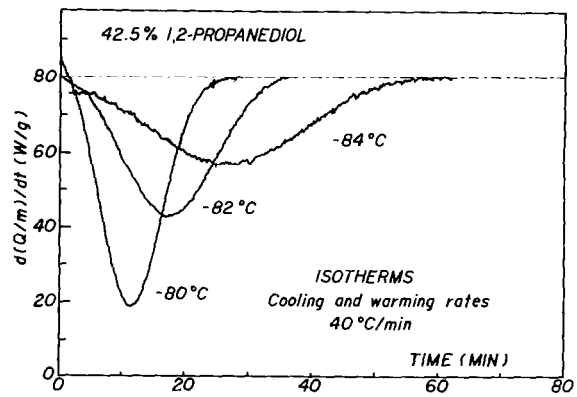

Fig. 6. Isothermal thermograms acquired by DSC-4 for 42.5% 1,2-propanediol in pure water. The sample is cooled at 40°C min^{-1} to −160°C as for Fig. 4 but is warmed back at the same warming rate, 40°C min^{-1}, to either −80, −82 or −84°C.

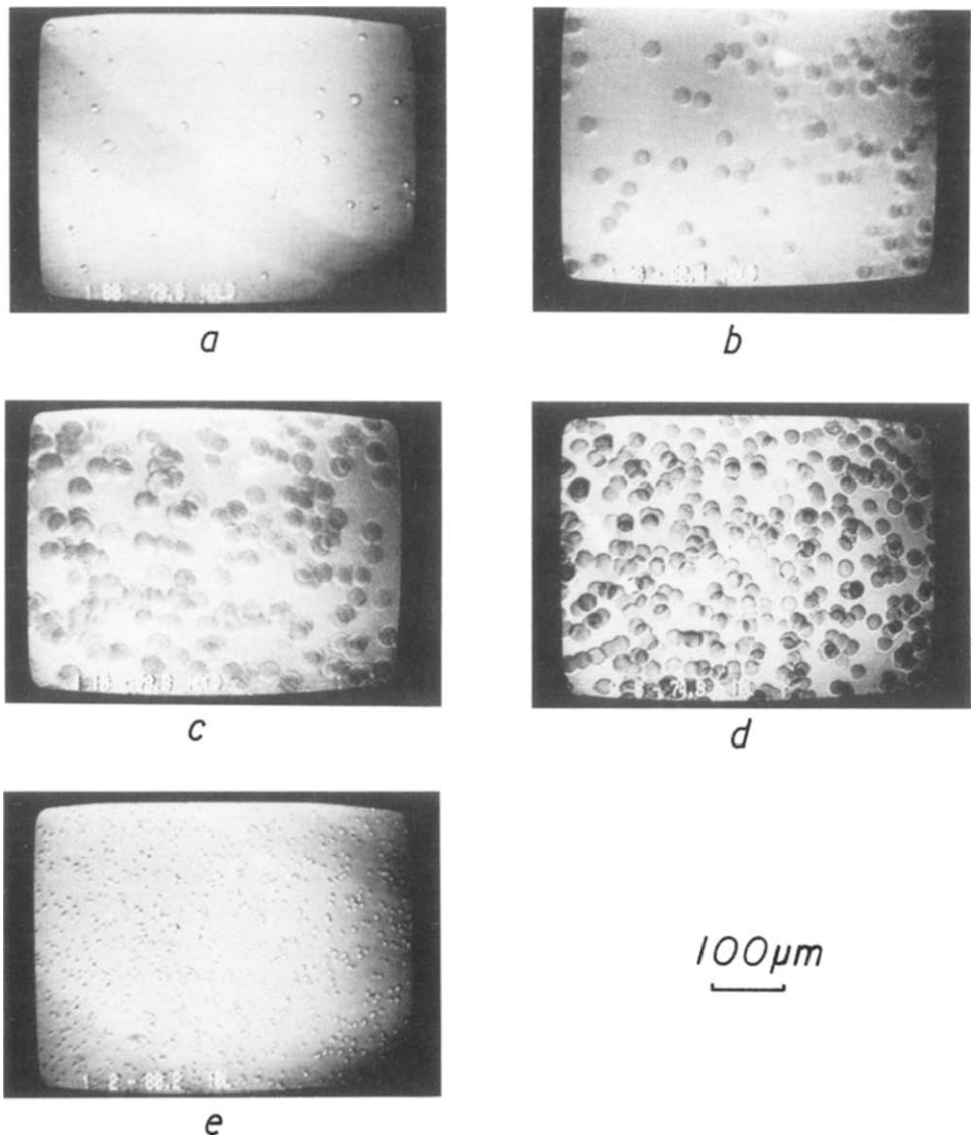

Fig. 7. Cryomicroscopy observation of the nuclei density for 42.5% 1,2-propanediol samples cooled at 40°C min^{-1} to −160°C and warmed at different warming rates V_w to temperatures higher than −80°C. V_w = (a) 80°C min^{-1}; (b) 40°C min^{-1}; (c) 10°C min^{-1}; (d) 5°C min^{-1} and (e) 2°C min^{-1}.

mental conditions as those of Fig. 5, demonstrating the growth of stable nuclei during the isotherms for different warming rates. Both the shape and size of each crystal are the same within the ability of the screen to resolve them.

In Fig. 8, the density of nuclei observed by cryomicroscopy has been determined for the same experimental conditions as in Fig. 7. Density is

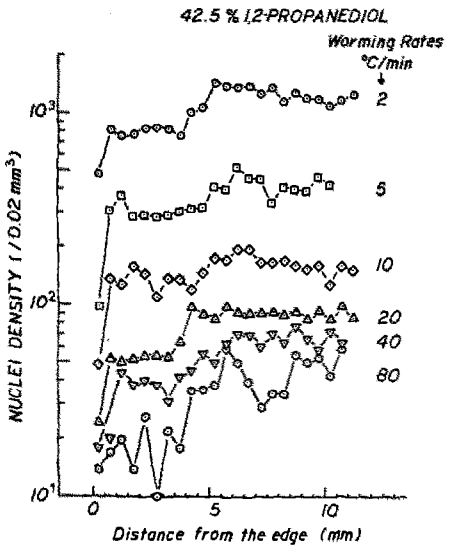

Fig. 8. Density of nuclei (nuclei per 0.02 mm^3) for 42.5% 1,2-propanediol counted from cryomicroscopy observations (as from Fig. 6) for each screen (corresponding to 0.02 mm^3 of solution) as a function of the distance from the edge of the sample. The sample is cooled at 40°C min^{-1} to −160°C and warmed at the different warming rates reported on the figure.

presented as the number of crystals in 0.02 mm^3 of solution (the volume observed on one TV screen). Figure 8 compares the density as a function of their distance from the sample edge. For a warming rate of 5°C min^{-1}, the thermal gradient through the sample is not large. Only the first two TV screen distances have a density significantly lower than the middle of the sample. For each warming rate, the mean value and the variance of the density in logarithmic scales are given in Fig. 9 as functions of the warming rate V in a logarithmic scale. For warming rates up to 20°C min^{-1}, the log of the density of the nuclei seems to vary linearly with the log of V with a slope close to −1.16. Over this range the density of the nuclei is therefore close to being inversely proportional to V. For higher warming rates, the density seems to decrease towards a limit of between 20 and 50 nuclei per 0.02 mm^3.

The same experiment was performed with different initial cooling rates down to −160°C but with the same warming rate of 40°C min^{-1} to −80°C. The density of nuclei is reported as a function of the initial cooling rate (Fig. 10). It is apparent that the dependence of the density on cooling rate is less than its dependence on the warming rate.

Similar calculations for nucleus density were performed for 45% 1,2-propanediol, and the results are presented in Fig. 11: 10–25 nuclei per 0.02 mm^3 is the limit achieved for this solution over the range of warming rates shown in the abscissa at an initial cooling rate of 40°C min^{-1}.

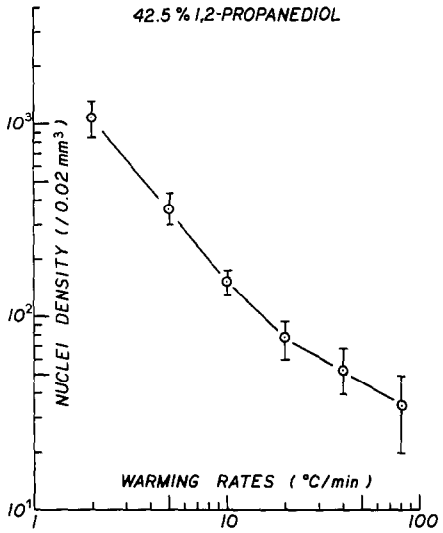

Fig. 9. Mean value and variance of the density of nuclei from Fig. 8 as a function of the warming rate. For warming rates up to 20°C min^{-1}, the variation is linear with a slope of −1.16, with a variance of 0.998 for the density mean values.

An analysis of the correlations between cryomicroscopy and DSC data are reported in Fig. 12 for the experimental conditions of Figs. 5 and 9, where the time t_{max}, as described previously, is plotted against the density of nuclei, both in logarithmic scales. The variation beween the log of t_{max}

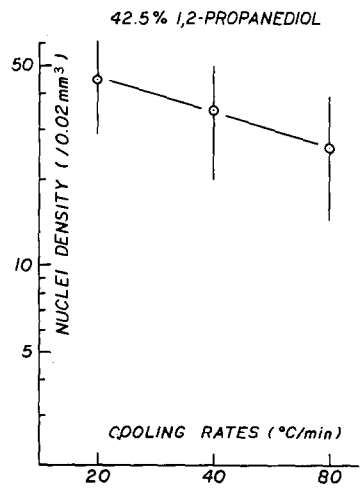

Fig. 10. Mean value and variance of the density of nuclei (nuclei per 0.02 mm^3) for 42.5% 1,2-propanediol as a function of the initial cooling rate when the sample is warmed back at 40°C min^{-1} to −80°C.

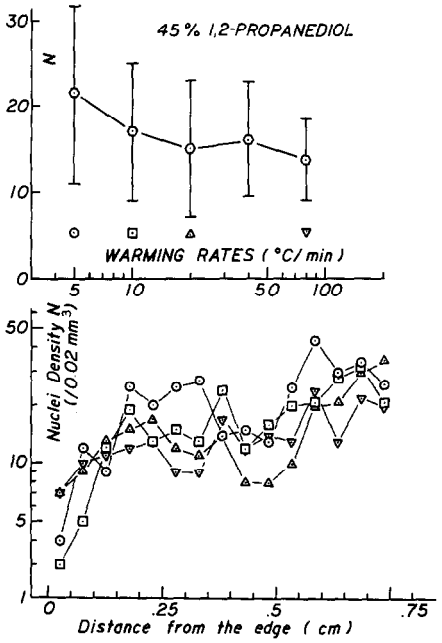

Fig. 11. Mean value and variance of the density of nuclei (nuclei per 0.02 mm^3) for 45% 1,2-propanediol as a function of the warming rate after the sample has been cooled at 40°C min^{-1} to −160°C.

versus the log of the density of nuclei is linear, with a slope of +0.46. The Arrhenius behavior of t_{max} is reported in Fig. 13 for 42.5% 1,2-propanediol where the samples are cooled at 40°C min^{-1} to −160°C and warmed at different warming rates. The slope of the linear variation is proportional to

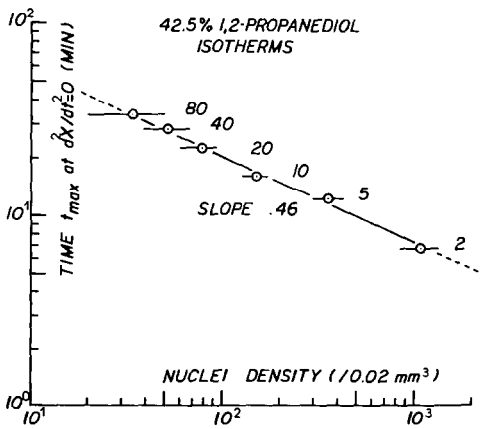

Fig. 12. Time t_{max} at the maximum of the crystallization rate ($d^2X/dt^2 = 0$) determined by calorimetry compared to the nuclei density determined by direct observations in the cryomicroscope. The linear variation has a slope of 0.46.

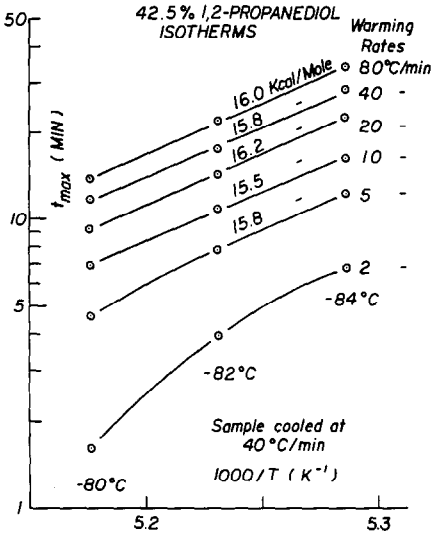

Fig. 13. Arrhenius plot of the time t_{max} of the maximum crystallization rate as a function of $1000/T$. The sample was cooled at 40°C min^{-1} to −160°C and warmed at different rates to temperatures T for the isothermal exposition. The slope is proportional to the activation energy E reported above the corresponding curves.

the activation energy E as defined previously [3,4] and is shown above each curve.

DISCUSSION

Comparison between cryomicroscopy and DSC

According to Figs. 1–4, both techniques, cryomicroscopy and DSC, show good agreement between direct optical observations and the thermal events recorded by DSC. Localizing the glass transition helps to interpret the fracture phenomenon which occurs well below the glass transition temperature. Direct observations of the fractures also assists in the interpretation of the anomalous behavior of the devitrification peak in DSC measurements, i.e. that the devitrification during warming may depend on the density of fractures as observed for different vitrified aqueous solutions [3–6]. Cryomicroscopy helps to localize the Ostwald ripening phenomenon which is characterized by darkening of the aqueous solutions [3,4] but which is a very low energy process not observed by DSC [25]. The two techniques are clearly complementary.

The sensitivity of the DSC-4 is higher than the 0.2 mW necessary to quantitate the thermal events that we see. However at very low temperatures, the cryomicroscope is more subject to thermal gradients due to the sample size. Calibrations can show, for a warming of 5°C min^{-1}, a gradient up to 2°C between the recorded and the real temperature for the melting

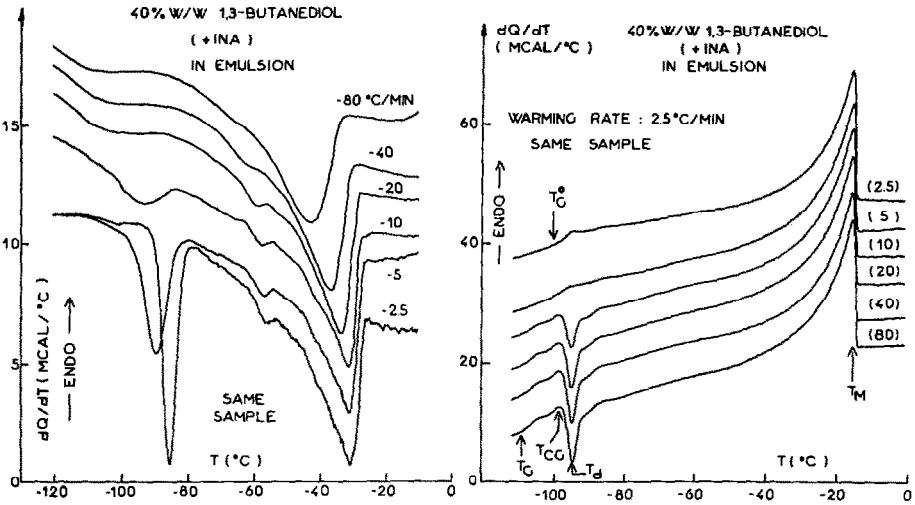

Fig. 14. Thermograms for an emulsion phase of 40% w/w 1,3-butanediol (from Fluka) in water containing INA measured on a DSC-4. On the left, thermograms during cooling are drawn for the different rates reported on the curve side. Two major exothermic peaks of crystallization appear for the lowest rates, corresponding to the homogeneous nucleation at the lowest temperatures and to the heterogeneous nucleation at the highest temperatures. On the right, thermograms on direct subsequent warming at 2.5°C min^{-1} are drawn with the initial cooling rate reported on the curve side corresponding to the thermograms of the left figure. Notations are the same as in Fig. 1.

of 2-propanol at −89°C (personal data). It is therefore important that there is an internal reference as in Fig. 4 where the end of melting is chosen as the reference point for both techniques.

Applications to the nucleation process

The separation between homogeneous and heterogeneous nucleation cannot be clearly defined, even with the extrapolation of the T_{hom} curve to the glass transition curve which has been determined only for a cooling rate of 2.5°C min^{-1}. Homogeneous nucleation is a kinetic phase separation between liquid and crystal phases and is a thermodynamic equilibrium process. However, when quenching experiments are done, the system is far from thermodynamic equilibrium. For these non-equilibrium states, molecules are subject to local diffusion rates based on the local viscosity of the solution at the local temperature. The present study, using combined techniques, supports the hypothesis that for emulsions of 1,3-butanediol–water solutions [26] (see Fig. 14) nucleation that occurs during cooling is stabilized during the subsequent warming although nuclei do not become visible below a certain temperature range. Other data, obtained with aqueous solutions of 44% 1,3-butanediol, where a vitrified sample undergoes a "homogeneous nucleation" at around −84°C during a warming at

10°C min^{-1}, show a discrete distribution of nuclei when the same vitrified sample is warmed at 80°C min^{-1} to different temperatures for isothermal measurements [3,4]. This observation is supported in the present work by the measure of nucleus density for 42.5% 1,2-propanediol as a function of the warming rate (Fig. 8).

The two sets of isothermal experiments described above and shown in the Figs. 5 and 6 support the fact that the history of the vitrification process is critical for the determination of the crystallization kinetics. Two factors are important: the cooling and warming rates for the nucleation process and the temperature of crystal growth. Indeed, the nucleation process is responsible for the thermal behavior recorded by DSC and reported in Fig. 5. The calculation of the density of nuclei from Fig. 8 shows that it is highly dependent on the warming rate and depends upon how far T_{hom} is from T_g. The linear dependence of nucleus density on the inverse warming rate is related to the proportionality of the number of nuclei formed during the time spent in the nucleation thermal domain by the sample during warming. In Fig. 7, all crystals have the same size and shape. Therefore it can be argued that the nuclei might have formed during cooling but were not able to be stabilized completely and to grow. This stabilization of nuclei occurs only during warming for concentrations higher than 40% 1,2-propanediol. It is notable in Fig. 10 that the dependence of nucleus density versus the initial cooling rate is less important. However, the nucleation process is highly concentration dependent.

For 45% 1,2-propanediol in Fig. 11, variation in density as a function of warming rate is negligible and for concentrations higher than 45%, the thermal history of the sample will have a limited effect on the ice crystallization during warming. The limited number of nuclei seen may be due to heterogeneous nucleation from impurities, as homogeneous nucleation is no longer a major influence. For 45% 1,2-propanediol, the limit of nuclei concentration is around 10^6 nuclei per cm^3. Further experiments are needed to be able to separate the two types of nucleation. For devitrification during warming for the same sample, only crystal growth by itself will affect the Arrhenius behavior of K.

According to the Johnson–Avrami theory, the product Kt_{max} is constant. For Fig. 12, because the final temperature is the same for the different warming rates used, $\exp(-E/RT)$ is assumed constant with E independent of the nuclei density. Therefore $K_0 t_{max}$ is constant. Then, because t_{max} is nearly inversely proportional to the square root of the density of nuclei, K_0 is nearly proportional to the square root of the density of nuclei. As already mentioned, for 1,3-butanediol [3,4] the constant K can be determined directly by observation of the growth of crystals. For specific cases, we have calculated that for a fixed number of stable nuclei N, K is proportional to $N^{1/n}$, where n is the Avrami exponent [3,4]. As seen in Fig. 7, the crystals seem to grow in a discoidal shape. This is in good agreement

with the variation of K_0 with the square root of the nucleus density. The independence of the activation energy E and the density of nuclei will have to be verified later.

For Fig. 13, where the isotherms were recorded at different temperatures for different warming rates, K_0 is assumed to be constant because the similarity of crystal size to that of Fig. 7 shows that the nucleation stabilization occurred at temperatures lower than −84°C: no additional nuclei can be formed during the isothermal exposure of the sample at temperatures higher than −84°C. Direct observation of the crystals by cryomicroscopy shows that the product $t_{max} \exp(-E/RT)$ is constant, as has already been proposed [3,4]. It must be emphasized that this is not true if nucleation proceeds during the isothermal exposure. Figure 13 gives the Arrhenius variation of t_{max} where, using warming rates higher than 5°C min^{-1}, the slope gives similar values for $E = 15.8 \pm 0.2$ kcal mol^{-1}. This shows that the activation energy E does not depend on the density of nuclei. It can also be seen in Fig. 13 that for warming rates of 2 and 5°C min^{-1}, the curves are concave to the axis of $1000/T$, because crystal growth has already begun at lower temperatures (−85°C for 2°C min^{-1} and −81°C for 5°C min^{-1}). Therefore the t_{max} has a value lower than expected.

CONCLUSIONS

The combination of cryomicroscopy and differential scanning calorimetry is uniquely useful. Cryomicroscopy, as a complementary technique to DSC, permits both qualitative and quantitative measurements. Our data on nucleation in relatively concentrated aqueous solutions of 1,2-propanediol is a good example, supporting predictions based on data with aqueous solutions of 1,3-butanediol [3,4]. Its role is, however, limited for aqueous solutions at particular concentrations where the homogeneous nucleation process can be kinetically limited.

Our observations indicate that the thermal history of the vitrified samples is critical to investigations of kinetics. Homogeneous nucleation is a kinetic process and the number of nuclei formed is dependent on thermal treatments. Nucleation can be induced and hidden during the vitrification of the solid but, at least for aqueous solutions of vitrification agents used for cryoprotection, stabilization of the nuclei will occur during rewarming where growth has not occurred during cooling. The concept of nucleus stabilization is important for the interpretation of devitrification, especially in cryoprotective aqueous solutions.

Cryomicroscopy also provides a good correlation with and support for the interpretation of kinetics parameters under isothermal conditions. Both the present paper and previous results [3,4] have shown, for 1,3-butanediol and 1,2-propanediol, that under isothermal conditions nucleus density does

not change during the isothermal exposure. However, it does change during the transient thermal processes used in our experiments, showing that even for isothermal experiments, experimental conditions must be defined. Comparison of crystallization kinetics between solutions must be in two steps: first the thermal dependence of the nucleation must be determined, after which the kinetics parameters can be analyzed for crystal growth in isothermal experiments.

For a binary system such as water–1,3-butanediol, difficulties arise in interpreting the kinetics parameters measured by thermal analysis under isothermal conditions. But cryomicroscopy helps in this attempt [3,4]. Its role may be even more important in theoretical models for crystallization kinetics in glasses during warming at continuous heating rates, as pointed out previously. Indeed, recognizing that nucleation is a function of the time spent by the sample in the nucleation temperature domain, the constant K_0 is no longer independent of time or of cooling and warming rates. The influence of the type of nucleation is already included in the Avrami exponent n in the mathematical treatment of the transformation [9]. However, in conditions where the nucleation process has no overlap with the crystal-growth thermal domain, as seen previously for relatively concentrated aqueous solutions of 1,2-propanediol and of 1,3-butanediol [26], most of the theoretical models do not take into account this type of nucleation. The present results show that while the assumption that K_0 is independent of time might be acceptable for cooling experiments, this will not be true for warming back from the vitrified state. A correction for the kinetics parameters under continuous heating-rate conditions must therefore be applied for the K_0, reflecting specific experimental conditions.

The simplest procedure will be to perform the calculations of MacFarlane et al. [10] and to substitute the precise nucleation rate with an oversimplified model with a Gaussian curve, such as $N = N_0 \exp(-(T - T_N)^2/2\sigma^2)$ where T_N is the temperature of maximum nucleation, σ the width of the distribution and N_0 the number of nuclei sites created per unit of time and volume during the previous cooling. The calculation of nucleation density for different warming rates gives $\sigma N_0 = \text{constant}$, with the determination of σ depending on the separation of the crystal growth and nucleation domain. For 42.5% 1,2-propanediol, $\sigma N_0 = 3.3 \times 10^6$ K nuclei s^{-1} mm^{-3}. However, a definitive determination of the three parameters will need more complex experiments, certainly including annealing at different temperatures with different cooling and warming rates using combined cryomicroscopy/DSC techniques.

ACKNOWLEDGMENTS

The author thanks Dr. H.T. Meryman for his continuous support and Dr. R.J. Williams for his scientific and technical support and for correcting

the manuscript. This work is supported by Grant BSRG 2 S07RR05737 and NIH Grant 5R01GM-17959-15.

REFERENCES

1 P.M. Mehl, Cryobiology, 27 (1990) 687.
2 P. Boutron, Cryobiology, 27 (1990) 55.
3 P.M. Mehl, Thermochim. Acta, 155 (1989) 187.
4 P.M. Mehl, Cryobiology, 27 (1990) 378.
5 R.J. Williams and D.L. Carnahan, Cryobiology, 27 (1990) 479.
6 R.J. Williams, P.M. Mehl and D.L. Carnahan, in C.Th. Smit Sibinga, P.C. Das and H.T. Meryman (Eds.), Cryopreservation at Low Temperature Biology in Blood Transfusion, Kluwer Acad. Pub., Dordrecht, 1990, pp. 71–86.
7 P. Boutron, in D.E. Pegg and A.M. Karow, Jr. (Eds.), The Biophysics of Organ Cryopreservation, Plenum Press, London, 1988, pp. 201–228.
8 P. Boutron and F. Arnaud, Cryobiology 21 (1984) 348.
9 J.W. Christian, in R.W. Cahn (Ed.), Physical Metallurgy, North-Holland, Amsterdam, 1965, pp. 443–539.
10 D.R. MacFarlane, R.K. Kadiyala and C.A. Angell, J. Chem. Phys. 79 (1983) 3921.
11 D.H. Rasmussen and A.P. MacKenzie, in H.H.G. Jellinek (Ed.), Water Structure at the Water–Polymer Interface, Plenum Press, London, 1972, pp. 126–145.
12 P. Boutron and A. Kaufmann, Cryobiology 15 (1978) 93.
13 J.H. Flynn, in Proc. 19th NATAS Conference, Boston, September 1990, pp. 381–388.
14 J.H. Flynn, in Proc. 19th NATAS Conference, Boston, September 1990, pp. 389–396.
15 D.W. Henderson, J. Non-Cryst. Solids, 30 (1979) 301.
16 H. Yinnon and D.R. Uhlmann, J. Non-Cryst. Solids, 54 (1983) 253.
17 C.A. Angell, in K.L. Ngai and G.B. Wright (Eds.), Relaxations in Complex Systems, National Technical Information Service, U.S. Department of Commerce, Springfield, VA, USA, 1988, pp. 3–11.
18 S. Charoenrein and D.S. Reid, Thermochim. Acta, 156 (1989) 373.
19 P. Boutron and A. Kaufmann, Cryobiology 16 (1979) 557.
20 R.C. Weast (Ed.), CRC Handbook of Chemistry and Physics, 70th edn., CRC Press, Boca Raton, 1989–1990, p. D-252.
21 D.H. Rasmussen and B. Luyet, Biodynamica, 10 (1969) 319.
22 P.M. Mehl and G.M. Fahy, Cryobiology, 27 (1990) 683.
23 G.N. Chapman and A.J. Walton, J. Appl. Phys., 54 (1983) 5961.
24 J.T. Dickinson, L.C. Jensen and M.R. McKay, J. Vac. Sci. Technol., A4(3) (1986) 1648.
25 D.R. MacFarlane and M. Forsyth, in D.E. Pegg and A.M. Karow, Jr., (Eds.), The Biophysics of Organ Cryopreservation, Plenum Press, London, 1988, pp. 237–263.
26 P.M. Mehl, Cryobiology, 27 (1990) 686.